Distribution Network Operation Under Uncertainty Using Information Gap Decision Theory

Alison O'Connell, *Student Member, IEEE*, Alireza Soroudi, *Member, IEEE*, Andrew Keane, *Senior Member, IEEE*

***Abstract*—The presence of uncertain parameters in electrical power systems presents an ongoing problem for system operators and other stakeholders when it comes to making decisions. Determining the most appropriate dispatch schedule or system configuration relies heavily on forecasts for a number of parameters such as demand, generator availability and more recently weather. These uncertain parameters present an even more compelling problem at the distribution level, as these networks are inherently unbalanced, and need to be represented as such for certain tasks. The work in this paper presents an information gap decision theory based three-phase optimal power flow. Assuming that the demand is uncertain, the aim is to provide optimal and robust tap setting and switch decisions over a 24-hour period, while ensuring that the network is operated safely, and that losses are kept within an acceptable range. The formulation is tested on a section of realistic low voltage distribution network with switches and tap changers present.**

***Index Terms*—Load flow, optimisation, power distribution, smart grids, three-phase electric power, uncertainty.**

I. Introduction

UNLIKE high voltage and medium voltage networks, low voltage (LV) distribution networks were not designed with any kind of control or management in mind. At present, LV networks are typically passive components of the power system, solely delivering power to the customer. However, the addition of new technologies to LV feeders, means that these networks may demand more proactive management in the future. Although control at high level is possible, it cannot consider LV constraints, such as voltage limits, and may result in operation outside safe operating bounds. Furthermore, it cannot provide control decisions for LV components. Concerns over the future of distribution networks have led distribution system operators to implement field trials and impact studies for distributed resources, such as electric vehicles, on their LV networks [1], [2]. Some of the studies described in [3] focus on utilising existing distribution equipment to improve the planning and operation of LV networks, and move towards a more active approach. Although gaining further control and observability of LV networks is desirable, it is not a trivial task. LV networks are unbalanced in nature due to the presence of single, two, and three-phase loads, and untransposed lines, therefore control methods for HV and MV networks that typically model systems using a balanced representation, are unsuitable for LV use. Furthermore, unlike HV and MV where demand is aggregated and easier to forecast, individual customer load can be quite difficult to predict [4] so the level of uncertainty at LV level can be quite significant. Therefore it is important to consider and model the LV network.

Various methods exist for dealing with the uncertainties in unbalanced distribution networks [5]. The work in [6] presents a probabilistic unbalanced load flow using a Monte-Carlo approach. The method is used on a distribution system that has wind turbines connected, taking the wind speed and active and reactive load as uncertainties. In [7] an interval arithmetic based unbalanced power flow is developed to manage uncertainties in both load and feeder parameters. Other works have made further progress with the incorporation of optimisation. [8] presents a rolling three phase load flow and optimisation formulation which minimizes the cost of electric vehicle (EV) charging. The method updates inputs to reduce the negative impacts of EV uncertainties. The authors in [9] have proposed a chance-constrained optimisation-based unbalanced optimal power flow (OPF) for use on radial distribution networks with distributed generation present. The multi-objective aims to minimize the active power losses, overloading, and voltage violations. In [10] a fuzzy unbalanced power flow with a genetic algorithm is used to control tap changers and the reactive power output of capacitors under load uncertainty. One of the objectives is to minimize active power loss. Distribution feeder loss minimisation under load uncertainty is also examined in [11] and [12].

Information gap decision theory (IGDT) [13] is a decision making method that has been utilized within various fields [14]–[17], and has recently been incorporated into power systems research to combat the problems caused by uncertainties. In [18], an IGDT-based approach is proposed to manage the revenue risk of the electric vehicle aggregator caused by electricity price uncertainties. The authors in [19] propose an IGDT-based technique to address the variability and uncertainty of renewable generation and to handle the congestion issue in distribution networks. The work in [20] uses IGDT to produce an energy procurement strategy for a network which has uncertain distributed generation present, while also taking account of network constraints.

As shown by the comparison of uncertainty formulations in Table I, IGDT is a decision making method that, unlike other methods, does not require knowledge of probability distributions, membership functions or detailed uncertainty sets. The lack of using probabilities does mean that performance is not maximized under expected conditions but rather

A. O'Connell (alison.o-connell@ucdconnect.ie), A. Soroudi and A. Keane are with the School of Electrical and Electronic Engineering, University College Dublin, Ireland. This work was conducted in the Electricity Research Centre, University College Dublin, Ireland, which is supported by the Commission for Energy Regulation, Bord Gáis Energy, Bord na Móna Energy, Cylon Controls, EirGrid, Electric Ireland, Energia, EPRI, ESB International, ESB Networks, Gaelectric, Intel, SSE Renewables, and UTRC.

A. O'Connell is funded under the Programme for Research in Third-Level Institutions (PRTLI) Cycle 5, and co-funded under the European Regional Development Fund (ERDF). A. Soroudi is funded through Science Foundation Ireland (SFI) SEES Cluster under grant number SFI/09/SRC/E1780.

performance is acceptable over a large range of conditions. It does not capture unexpected events, however, it is capable of modeling severe uncertainty without significantly increasing the complexity of the underlying problem. Furthermore, IGDT guarantees that the objective will not exceed a predefined value. The simplicity and reliability of the method make it ideal for incorporation into unbalanced distribution network analysis, as it can account for the considerable uncertainty that distribution networks face, without increasing the computational burden of an already intricate formulation.

Table I
COMPARISON OF UNCERTAINTY METHODS

The work presented here utilizes the IGDT method in conjunction with the three-phase OPF (TOPF) developed in [21] giving a robust TOPF. The TOPF itself is not the main contribution, however, it is a core part of the formulation. For the purposes of this work, this novel method will be used as an operational tool to provide network operators with robust day ahead decisions for a particular LV network. The focus of this work is to deal with the uncertainty of apparent power demand in the network. The TOPF and IGDT method assesses the level to which demand can vary from its predicted value, for a given acceptable variation in the optimal predicted losses, while ensuring that the network is operating within its safe technical limits. The contributions of this paper are threefold:

- Developing a single IGDT TOPF formulation to provide optimal and robust decisions for distribution system control variables.
- Using IGDT to model the uncertainty of demand with limited available data, and guaranteeing the value of losses.
- Accurately modeling the distribution system using a three-phase unbalanced approach.

The paper is organized as follows: The methodology is outlined in Section II, a detailed description of the test case is given in Section III, Section IV outlines the main results and conclusions are presented in Section V.

II. METHODOLOGY

A. Information Gap Decision Theory

IGDT is a method for decision making under severe uncertainty. An information gap refers to the discrepancy between what is known and what is possible. In the context of power system uncertainty, the information gap describes the disparity between the operating point that the decision maker deems most likely, and the actual operating point, which is unknown. IGDT uses nested sets, with each set defining a particular information gap level, and each element representing a possible operating point.

The required input for IGDT is an initial prediction of what the values of the uncertain parameter will be. Decision makers can then assess either a robustness function or an opportuneness function. The robustness function indicates the maximum allowable deviation from the predicted value, in an undesired direction, while maintaining an acceptable deterioration in the objective value. The opportuneness function indicates the minimum required deviation from the predicted value, in a desired direction, which will result in an anticipated improvement in the objective value. The uncertain parameter belongs to an uncertainty set U which is defined in (1-3). In contrast to robust optimisation or interval based mathematical modeling, the uncertainty set used in IGDT is not precisely known. In fact, it is also subject to uncertainty. The uncertain parameter is represented by Λ. The only information available regarding Λ is its predicted value $\bar{\Lambda}$. The α in (1-3) is called the radius of uncertainty. It describes the deviation of the actual uncertain parameter values from the predicted values. Since the actual value of the uncertain parameter is unknown, α is also unknown.

$$U(\alpha, \bar{\Lambda}) = \left\{ \Lambda : \left| \frac{\Lambda - \bar{\Lambda}}{\bar{\Lambda}} \right| \leq \alpha \right\} \tag{1}$$

$$0 \leq \alpha \tag{2}$$

$$\Lambda \in U(\alpha, \bar{\Lambda}) \tag{3}$$

The objective of the IGDT problem is to find the tolerable radius of uncertainty, $\hat{\alpha}$, i.e. the gap between the predicted value of the uncertain parameter and the maximum/minimum value that the system can tolerate/expect. In order to solve the robustness problem $\hat{\alpha}$ is maximized, while the opportuneness problem is assessed by minimizing $\hat{\alpha}$. This is achieved by incorporating $\hat{\alpha}$ into an optimization as a decision variable. Fig. 1 gives a description of the IGDT formulation for the robustness problem. α_{max} can only be reduced by using better prediction techniques. The IGDT method, however, does not aim to reduce the uncertainty, but rather tries to increase the tolerable uncertainty, $\hat{\alpha}$, by finding the optimal settings for decision variables.

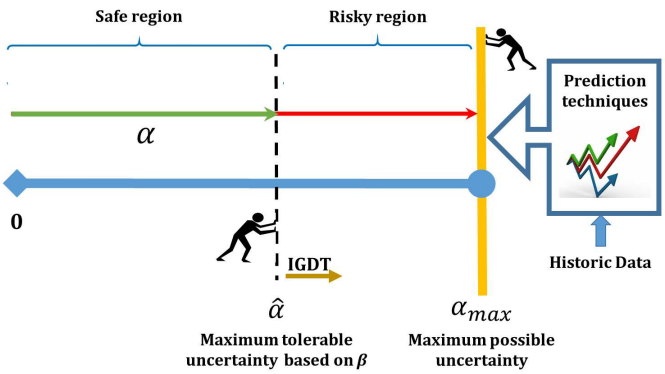

Figure 1. Description of IGDT for robustness

A comprehensive description of the IGDT method can be found in [13] and [22], which include theoretical definitions

of both the robustness and opportuneness algorithms, various model descriptions, and detailed worked examples.

B. Network modeling in the TOPF

The three-phase optimal power flow (TOPF) method incorporates three phase unbalanced load flow to an optimisation program. The formulation allows for the integration of all of the different elements that are inherent to unbalanced distribution networks, such as capacitors, ZIP loads and voltage regulators and is capable of modeling both radial and meshed networks. It can be used as either a planning or operational tool to model and provide optimal solutions for three-phase unbalanced distribution networks. A detailed description of the TOPF formulation can be found in [21], however a basic overview is given in the following subsections. Symbols shown in bold represent phasors, while non-bold symbols indicate scalar values.

1) Power Flow: The three-phase power flow equations are implemented as equality constraints, where the real and imaginary current mismatches at bus k phase d, and the real and imaginary current mismatches at bus k neutral phase, are constrained to equal zero as in (4). Definitions for these mismatches can be found in [21].

$$\Delta I^d_{Re_k} = \Delta I^d_{Im_k} = \Delta I^n_{Re_k} = \Delta I^n_{Im_k} = 0 \tag{4}$$

where
$k \epsilon \Omega$ Ω : set of buses;
$d \epsilon \Omega_d$ Ω_d : set of phases $\{a, b, c\}$.

2) Loads: Loads are modeled using the composite ZIP representation. This means loads are represented by a composition of three different types of load; constant impedance load (Z), constant current load (I), and constant power load (P). The proportions of each type of load utilized are determined by the voltage dependence of the load [23]. The specified active and reactive power demand, $P^d_{D_k}$ and $Q^d_{D_k}$ respectively, are given in terms of their ZIP components in (5) and (6).

$$P^d_{D_k} = P^d_{P_k} + P^d_{I_k}\left|V^d_k - V^n_k\right| + P^d_{Z_k}\left|V^d_k - V^n_k\right|^2 \tag{5}$$
$$Q^d_{D_k} = Q^d_{P_k} + Q^d_{I_k}\left|V^d_k - V^n_k\right| + Q^d_{Z_k}\left|V^d_k - V^n_k\right|^2 \tag{6}$$
$$\mathbf{S^d_{D_k}} = P^d_{D_k} + jQ^d_{D_k} \tag{7}$$
$$P^d_k = P^d_{G_k} - P^d_{D_k} \tag{8}$$
$$Q^d_k = Q^d_{G_k} - Q^d_{D_k} \tag{9}$$

where

$P^d_{D_k}$,$Q^d_{D_k}$, $\mathbf{S^d_{D_k}}$	active, reactive and apparent demand at bus *k* phase *d*;
$P^d_{P_k,I_k,Z_k}$,$Q^d_{P_k,I_k,Z_k}$	ZIP model components of active and reactive power at bus *k* phase *d*;
P^d_k,Q^d_k	specified active and reactive injection at bus *k* phase *d*;
$P^d_{G_k}$,$Q^d_{G_k}$	active and reactive generation at bus *k* phase *d*.

3) Tap Changers and Voltage Regulators: A detailed discussion of how tap changers are modeled in this formulation is given in [21] and will not be repeated here. However, the key voltage equation is shown in (10), where r^d_{ik} refers to the turns ratio at phase d between buses i and k. The turns ratio refers to the ratio of the number of winding turns on the primary side of a transformer, to the number of turns on the secondary side.

$$\mathbf{V^d_k} = r^d_{ik} \times \mathbf{V^d_i} \tag{10}$$

In order to reduce computational burden, the turns ratio, and therefore the tap settings, are modeled as a continuous variable in the main TOPF iteration. Continuous modeling of tap settings is suggested by the authors in [24] and has been utilized in other works such as [25]. To ensure that tap settings are modeled accurately, the resulting tap settings are then rounded to the nearest integer and modeled as a parameter. A second TOPF iteration is then performed to confirm that the new integer tap settings provide a valid solution and do not result in any constraint breaches. Although the rounded tap settings may not be optimal, they provide a more realistic representation of actual tap settings. This should eliminate the need to introduce integer modeling to the formulation. The tap settings will be analysed as part of the results to confirm the assumption that the continuous modeling is appropriate.

4) Switches: In order to find optimal switch settings, a configuration dimension has been introduced to the TOPF, where Ω_m is the set of configurations. The objective is then minimized or maximized over all configurations, time steps, buses and phases. The optimal configuration for each time step is subsequently identified by comparing the configurations at each time step, and determining which gives optimal objective value. This determines whether switches are open or closed.

5) Ratings: Equipment and network ratings are also accounted for in this work. Equations describing these ratings are given in [21], and will not be repeated here.

C. Formulation

The IGDT based TOPF is used as a day ahead operational tool for the purposes of this work. The method can provide the system operator with robust and optimal setpoints for network control variables. These set-points will allow the network to be operated in such a way that deviations in the uncertain parameter will not cause any technical limits to be breached, and will not cause the objective to vary by more than a specified value.

The uncertain variable in this work is the apparent power demand $S^d_{D_k}$, where $\bar{S}^d_{D_k}$ is the predicted value for demand. The predicted value for demand could be made using historical demand data for the particular feeder. The primary objective is to minimize the losses. Losses are caused by energy flow through the lines. These flows are dependent on demand, therefore if demand is uncertain then losses are also uncertain. The following steps describe the proposed solution procedure:

Step 1: Calculate the predicted optimal active power losses $\bar{P}_L$. A deterministic TOPF, using the predicted values for the demand, $\bar{S}^d_{D_k}$, is performed to obtain a

predicted value for the losses. This is the amount of losses that the network operator will face if there is no demand uncertainty. The set of equations in (11) should be solved to obtain $\bar{P}_L$.

$$\begin{aligned} & f = \sum_{m\epsilon\Omega_m} \sum_{h\epsilon\Omega_h} \sum_{k\epsilon\Omega} \sum_{\substack{i\epsilon\Omega_k \\ i\neq k}} \sum_{d\epsilon\Omega_d} (P^d_{L_{ki}})^m_h \\ & \bar{P}_L = \min f \\ & \hat{\alpha} = 0 \\ & \mathbf{S^d_{D_k}} = \bar{\mathbf{S}}^{\mathbf{d}}_{\mathbf{D_k}} \\ & \text{Subject to TOPF constraints} \end{aligned} \tag{11}$$

where

$P^d_{L_{ki}}$	the active power losses between buses i and k for phase d;
Ω_h	set of time steps;
Ω_k	set of buses connected to bus k;

Step 2: Repeat with tap settings set as an integer parameter (as discussed in Section II-B3).

Step 3: Set the tolerable limit of the losses, P_{L_c}, when the demand uncertainty exists in the model. The limit P_{L_c} is set as a percentage of the predicted losses using a new parameter, β, known as the tolerable loss variation. This means that, depending on whether robustness or opportuneness is being assessed, it is acceptable for losses to be either $1+\beta$ times larger (robustness) or $1-\beta$ times smaller (opportuneness) than the predicted value $\bar{P}_L$, as in (12). The value of β can be chosen by the system operator, and could be determined using historical data, or a predefined feeder loss limit.

$$P_{L_c} = (1 \pm \beta)\bar{P}_L \tag{12}$$

Step 4: Depending on whether robustness or opportuneness is being analysed, perform a new iteration of the TOPF either maximising or minimising the tolerable radius of uncertainty variable, $\hat{\alpha}$. This is achieved by solving the set of equations in (13), using $\max \hat{\alpha}$ and $1+\hat{\alpha}$ for robustness, or $\min \hat{\alpha}$ and $1-\hat{\alpha}$ for opportuneness.

$$\begin{aligned} & \max \,/\, \min \hat{\alpha} \\ & f \leq P_{L_c} \\ & \mathbf{S^d_{D_k}} = (1 \pm \hat{\alpha})\bar{\mathbf{S}}^{\mathbf{d}}_{\mathbf{D_k}} \\ & \text{Subject to TOPF constraints} \end{aligned} \tag{13}$$

Step 5: Repeat with tap settings set as an integer parameter (as discussed in Section II-B3).

Step 6: If desired, repeat steps 2-5 using different values for the tolerable loss variation β. This allows the network operator to assess how the tolerable radius of uncertainty $\hat{\alpha}$ is affected by changes in β, and therefore make more informed decisions about the appropriate operating point.

Step 7: Finish.

Using only an initial demand prediction, the results from steps 1-7 will provide the system operator with a range of set points for the switch and tap settings that will guarantee that the losses do not exceed the specified optimal value, provided the demand does not exceed the value given by $\hat{\alpha}$. Furthermore, the accuracy of the three-phase modeling will ensure that the network is operated in a safe manner at all times.

It is worth noting that it is not necessary to repeat steps 2-5. If the system operator knows the specific increase in losses that they are able to tolerate, then only one value of β needs to be assessed and steps 2-5 need only be performed once. Similarly, if the system operator has information regarding the error in the prediction of the demand, then fewer repeats of steps 2-5 may suffice, or the information may used to bound the value of $\hat{\alpha}$. However, the assumption in this work is that the system operator has limited knowledge about the demand, therefore a large range in β values, and subsequently $\hat{\alpha}$ values, will be analysed in this work.

The $\hat{\alpha}$ value obtained in step 4 is optimal due to the integration of the TOPF. It is possible to compute a unique value of $\hat{\alpha}$ for each customer load, by adding a new dimension to the $\hat{\alpha}$ variable, however, doing so would not provide any additional benefit. The smallest $\hat{\alpha}$ would be the limiting value for feeder, and that is what is captured by the formulation presented here.

The method is formulated as a non-linear program (NLP). The formulation has been implemented using AIMMS [26] optimisation modeling environment, and is solved using the non-linear programming solver CONOPT [27]. The stop criteria for the optimisation is given by CONOPT's default optimality tolerance value of 1×10^{-7}. It is worth noting that the problem is a non-convex one, therefore solutions may be locally, rather than globally, optimal.

III. Test Case

A. Test Network

The network utilized in this work is a section of actual LV network provided by the Irish DSO [28]. It represents a typical suburban network in Ireland. A detailed diagram of the network is given in Fig. 2. The network consists of two radial feeders, *feeder A* and *feeder B* shown by the dashed boxes in Fig. 2, that can be connected through a switch located at the end of each feeder. In this work, when the switch is open the network will be referred to as *radial*, and when the switch is closed it will be referred to as *meshed*. The distribution transformers at the beginning of each feeder also have tap changing capabilities. *Feeder A* has a total of 63 nodes, 9 three-phase nodes (including the transformer MV and LV nodes), and 54 single-phase customer nodes. *Feeder B* serves a total of 60 nodes, 8 three-phase nodes, and 52 single-phase customer nodes, giving a total of 123 nodes for the network as a whole. Each customer load and single-phase cable is modeled individually on its corresponding phase, and is given by an arrow in Fig. 2. The three phase nodes are named in Fig. 2 as *a1-a7* and *b1-b6*.

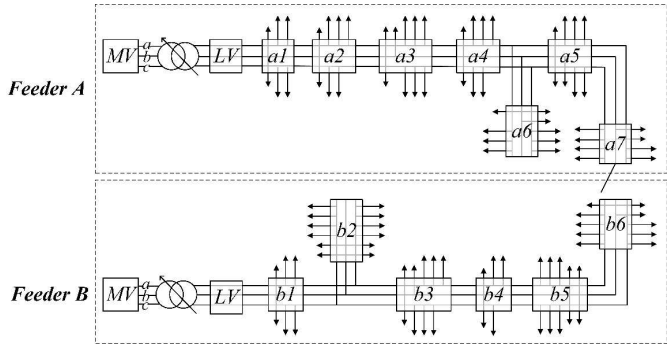

Figure 2. Diagram of 123 node practical test network

B. Demand Profiles

Demand profiles were generated using the residential load modeling tool described in [29]. The demand profiles were generated for a high load Winter day giving the worst case scenario for demand increases. The demand profiles are for a 24 hour period in 30 minute time steps, giving 48 time steps, and consist of active and reactive power, *Z* load component, *I* load component and *P* load component values for each customer and time step. The 30 minute time step ensures that control equipment has a sufficient amount of time to reach the given operating point. These demand profiles are used as the predicted values for apparent power demand. Sample active and reactive power profiles for three of the customers on the feeder are given in Fig. 16. The *ZIP* load components for a customer located at node a1 in Fig. 2 are shown in Fig. 17

C. Simulation Cases

The TOPF and IGDT method, as described in Section II, is used to determine optimal and robust tap and switch settings for the test network, for a 24-hour period in 30-min time steps, with the objective of minimising active power losses. The uncertain variable is the apparent power demand, and there are two simulation cases. The first case represents LV network demand at present, and assumes that all customers have similar demand uncertainty. The second case assesses a future scenario where certain customers are involved in demand response and therefore have a more significant level of demand uncertainty than other customers. Both cases are discussed further in the following subsections. Sample active and reactive power profiles as well as ZIP load components are given in Fig. 16 and Fig. 17 in the Appendix.

1) Full Uncertainty Case: The full uncertainty case assumes that all of the apparent power demand is uncertain. The robustness problem is formulated as in Section II-C but with a larger number of IGDT iterations using increasing values of the tolerable loss variation β. This allows the system operator to choose the operating point which has the required level of robustness against demand increases.

2) Demand Response Uncertainty Case: The demand response uncertainty case assumes that a number of customers on the test network are participating in a demand response scheme [30]. 25 customers have been chosen at random points along the test network shown in Fig. 2. These customers all have flexible demand that can be controlled by a third party operator, when necessary, to alleviate system wide issues. As it is assumed that demand response decisions are not managed by the distribution system operator, participating customers are therefore more likely to have a higher level of uncertainty associated with their demand, from a system operator perspective. Therefore, for this case it is assumed that only the demand response customers' apparent power demand is uncertain. Both the robustness and opportuneness functions are assessed in this case.

IV. Results and Discussion

The following subsections present the results for the two test cases. These results primarily present what a network operator would be concerned with, e.g. the control variable setpoints.

A. Full Uncertainty Case

This case assumes that all of the demand on the test network is uncertain. Fig. 3 shows the resulting tolerable radius of demand uncertainty $\hat{\alpha}$ values for the corresponding tolerable loss variation β values. It is clear that there is a relatively proportional relationship between allowable active power loss increases and apparent power demand increases. However, the demand cannot increase as much as the losses can. In fact, the $\hat{\alpha}$ values are less than half of the β values, and this ratio decreases as β increases further.

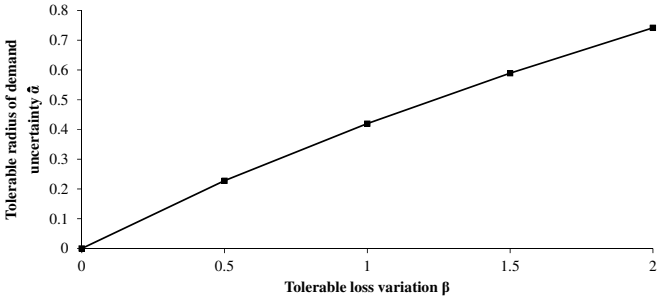

Figure 3. Tolerable radius of demand uncertainty $\hat{\alpha}$ vs tolerable loss variation β

Fig. 4 depicts the status of the switch that connects feeders A and B, for each time step. A dark box indicates that the switch is closed, while a light box represents the switch being open. All values of β resulted in the same switch settings, therefore only one is shown which represents all β values analysed. The optimal configuration does not change as β increases, as all of the load on the network increases uniformly. The switch is predominantly in the closed position showing that the *meshed* configuration is optimal in terms of losses for the majority of time steps. There is a window of time during the morning, however when the optimal switch position is open.

The resulting tap settings for the tap changers on feeders A and B are given in Fig. 5. The results given are for the phase a tap settings when β=0 and β=2. Phases b and c and other β values were also calculated but are not given here.

Figure 4. Switch status for each time step for all values of the tolerable loss variation β

The difference in the tap settings between β=0 and β=2 is relatively small, with the tap settings for β=2 set slightly higher than β=0, due to voltage drops experienced as a result of the increase in demand. Comparing feeders A and B it is clear that the tap settings are quite similar throughout the day. The only times that the tap settings on the two feeders are significantly different, are when the switch is open as shown in Fig. 4.

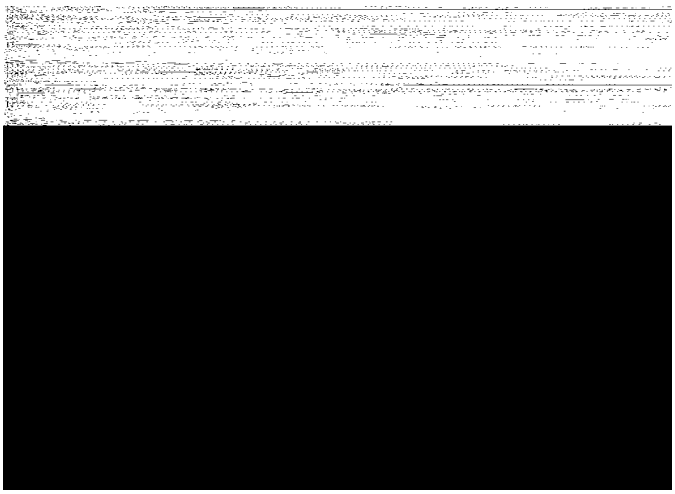

Figure 5. Tap settings for phase a of the tap changers on feeders A and B for β=0 and β=2

The optimal switch settings seen in Fig. 4 are reflected in the loss comparison presented in Fig. 6. This figure shows the percentage difference in the total losses between fully *radial* network configuration and the optimal configuration (from Fig. 4), given in light grey, and fully *meshed* configuration and the optimal configuration, given in black. It is clear that both fully *radial* and fully *meshed* operation produce higher losses than the optimal case, however fully *radial* operation gives losses approximately 1.6% higher than optimal for all values of β. This results in the largely *meshed* operation observed in Fig. 4.

Fig. 7 presents the aggregate apparent power load for each feeder, given by the solid line, as well as the actual imported apparent power at the source node of each feeder, given by the dashed line. The values shown here are for the *meshed* configuration when $\beta = 0$. Generally, *feeder A* imports more power than its load requires, which is to be expected due to losses. However, *feeder B* imports less power than its load requires. In fact, even during times when the *feeder B* load is larger than the *feeder A* load, for example from 10:30-12:00 or 15:00-16:30, *feeder B* still imports less than its load requirement. This indicates that, generally, *feeder B* experiences higher losses than *feeder A*, which again explains why *meshed* is more often the optimal operation choice than the *radial* for this network.

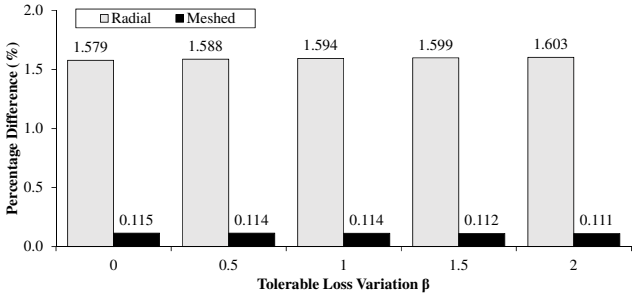

Figure 6. Percentage difference in the total losses between the optimized and radial configurations, and the optimized and meshed configurations

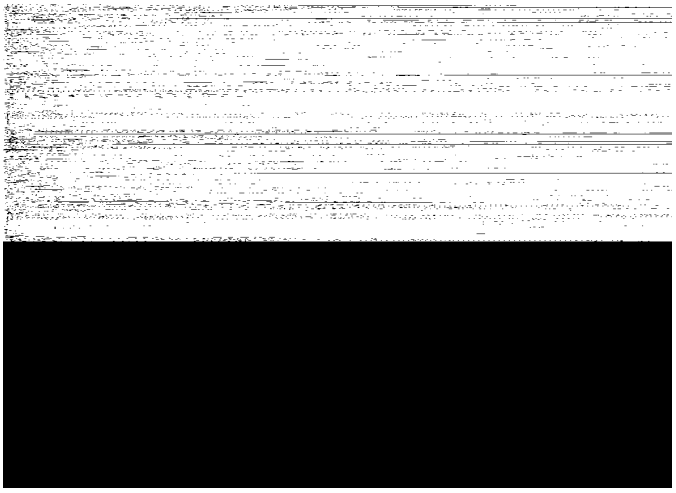

Figure 7. Aggregate apparent power demand for each feeder vs the apparent power imported at the source node of each feeder in the meshed configuration

Using these results, the system operator can decide which tap and switch settings to use. If the system operator decides to operate the feeders using the settings for β=0, they are taking the biggest risk in terms of safe feeder operation, but will have the lowest loss value if the actual demand is equal to the predicted value. Conversely, if the system operator implements the settings for β=2, they are reducing their risk level but will incur higher losses if the actual demand is equal to the predicted value. Given the results shown here, the decision maker can choose their control actions based on the results shown in Fig. 3. From this figure, they can find the balance between how much demand uncertainty they want their system to be able to tolerate, as well as the losses they are willing to incur. The best choice can be made using techniques such as fuzzy satisfying methods [31] which can find the best trade-off between the risk of demand increase and the expense of loss increase. The control results that correspond to the chosen data point should be the actions that the system operator implements.

B. Demand Response Uncertainty Case

The demand response uncertainty case targets the customers who are participating in a wider demand response scheme and assesses the uncertainty associated with their apparent power demand. Due to the nature of demand response, i.e. load can be either increased or decreased depending on the needs of the system, both the robustness and opportuneness functions are assessed in this case. The resulting values for the tolerable radius of demand uncertainty, $\hat{\alpha}$, are given for the corresponding tolerable loss variation, β, values in Fig. 8. The β values are still in reference to the total network losses in this case. Values to the left of the dashed line represent the opportuneness function while values to the right represent the robustness function, with the zero value being the base case. There is more scope for robustness as further increases in β in the direction of opportuneness would require these customers to generate power, i.e. their load values would need to be negative, which would be possible if they had grid connected micro-generation, however that is not considered in this work. It should also be noted that the $\hat{\alpha}$ values are much higher in this case than in the full uncertainty case, as there are fewer customers with uncertain load, therefore their load can be increased significantly more. In the figures that follow Fig. 8, β values for the opportuneness function will be presented as negative values.

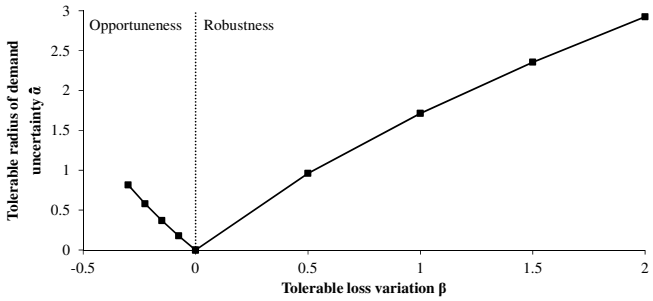

Figure 8. Tolerable radius of demand uncertainty $\hat{\alpha}$ vs tolerable loss variation β

Fig. 9 shows the total demand for the demand response customers. The predicted demand is given by the solid line, the dashed line shows the demand for $\beta = -0.3$ and the dotted line shows the demand for $\beta = 2$. It is evident that for losses to be reduced to 0.7 times their base value, i.e. $\beta = -0.3$, it is necessary for the demand response customers' total demand to be close to zero. As seen in Fig. 8, allowing the losses to increase threefold, i.e. $\beta = 2$, means that the aggregate demand for these customers can be almost 4 times larger than the initial predicted value, i.e. $\hat{\alpha} \approx 3$.

The switch status for the demand response case is presented in Fig. 10. Unlike the fully uncertain case, there is more variation in the switch settings in this case due to the fact that only the demand response customers' loads are considered uncertain. The difference between the load on *feeder A* and *feeder B* determines whether *meshed* or *radial* operation is optimal. *Radial* operation will be optimal when this difference is small, whereas *meshed* will be optimal when it is large. At

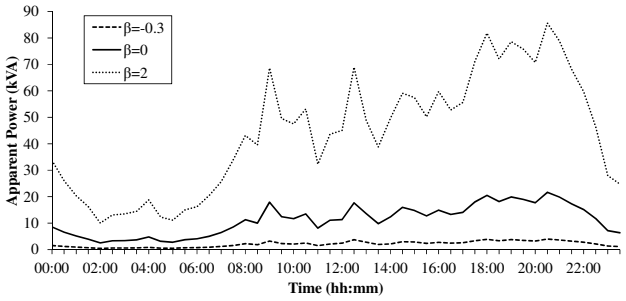

Figure 9. Aggregate load for demand response customers for varying levels of tolerable loss variation β

certain time steps, although the β values mean that overall load is lower than in the base case, the difference between the *feeder A* and *feeder B* load is more significant, leading to *meshed* operation. This also occurs in reverse at higher β values.

Figure 10. Switch status for each time step for increasing values of the tolerable loss variation β

The resulting phase a tap settings for the demand response case are given in Fig. 11. There is much more variation in the tap settings between β=0 and β=2 than previously seen in Fig. 5 for the full uncertainty case. Most of these variations are increases due to the increased level of demand. There is also a significant variation in the tap settings on feeders A and B. Both of these differences can be attributed to the switch settings shown in Fig. 10. There is generally more *radial* operation in this case in comparison to the previous case, and the switch settings change as β increases which does not occur in the fully uncertain case.

Fig. 12 shows the percentage difference between the *radial* and *meshed* losses and the optimal losses. In a similar fashion to the fully uncertain case, the percentage difference between the *radial* and optimal losses is much higher than that of the *meshed* and optimal. Deviation from the base case increases

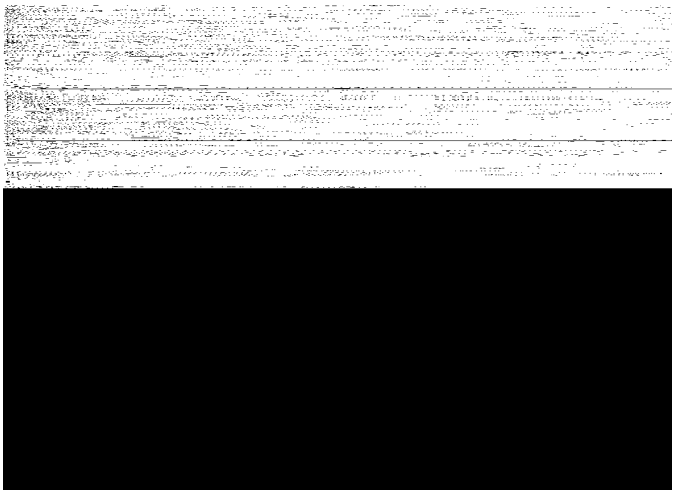

Figure 11. Tap settings for phase a of the tap changers on feeders A and B for β=-0.3, β=0 and β=2

the difference between the *radial* and optimal losses regardless of what direction that deviation moves. The difference in the *meshed* and optimal losses increases as β increases which is to be expected as the overall load increases. These results correlate to the switch settings seen in Fig. 10.

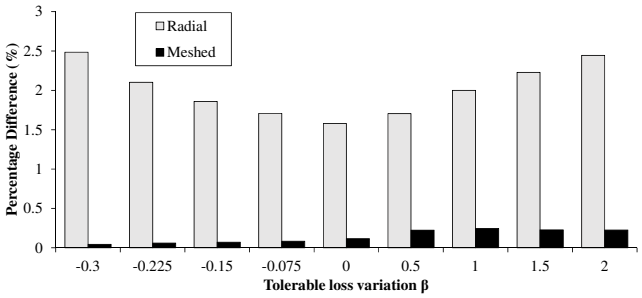

Figure 12. Percentage difference in the total losses between the optimized and radial configurations, and the optimized and meshed configurations

An alternative random selection of 25 customers was chosen for the demand response scheme and the formulation was performed again for the purposes of illustration. The resulting tolerable radius of demand uncertainty, $\hat{\alpha}$, values are compared to the $\hat{\alpha}$ values for the original customer selection in Table II. The original values are given by $\hat{\alpha_1}$ while the new values are called $\hat{\alpha_2}$. It is clear that although the customers participating in the demand response scheme have changed, the $\hat{\alpha}$ values do not vary significantly.

Table II
COMPARISON OF $\hat{\alpha}$ VALUES FOR TWO DIFFERENT SETS OF DEMAND RESPONSE CUSTOMERS

It is worth noting that, for all of the above cases, the difference between the total losses when the tap settings are modeled as a continuous variable, and when they are modeled as an integer parameter, is zero. This is due to the fact that the difference between the continuous and integer tap settings is small and thus has a negligible effect on the feeder. This indicates that, for LV networks similar to the test network used in this work, continuous modeling of tap settings should be sufficient.

The results presented show that changes in demand, be it increases or decreases, can significantly vary the optimal operating point of a network. However, the switch and tap settings provided by the TOPF and IGDT method allow system operators to be sure that their network is robust against these changes. This means that when the setpoints provided by the formulation are implemented, demand variations will not result in any voltage, current, or power limit breaches, and will not increase the minimized losses more than the value specified by the tolerable loss variation.

C. Convergence

Convergence of the formulation was analysed by solving the IGDT TOPF problem using the CONOPT solver, for the full load uncertainty case, for 100 different predicted load scenarios, using a β value of 1. The results in Table III show the convergence, as well as the iterations and computation time, for each of the 100 scenarios. The results show that all 100 scenarios converged, with a mean computation time of 325 seconds.

Table III
CONVERGENCE DATA FOR DIFFERENT PREDICTED LOAD SCENARIOS

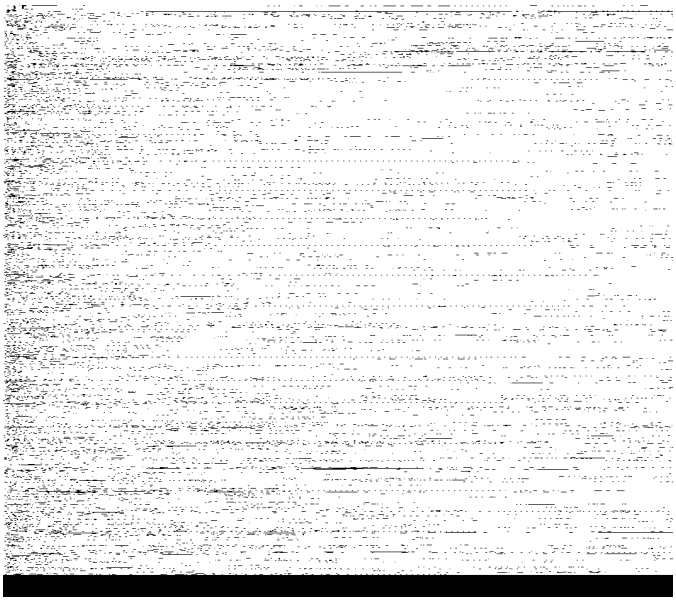

Table IV shows the convergence status, iterations, time and $\hat{\alpha}$ value for the full uncertainty case, using one predicted load value, for β=1, using three different NLP solvers that are available with AIMMS. The problem converged for all three solvers with similar computation times.

Table IV
CONVERGENCE DATA FOR DIFFERENT SOLVERS

D. Result Validation

In order to validate the results, the full uncertainty case from Section IV-A is considered at β=2. The corresponding $\hat{\alpha}$ results from Fig. 3 indicate that by implementing the resulting tap and switch settings, the demand can be up to 1.74 times the predicted value without increasing the losses by more than 3 times their predicted value. Three times the predicted value of losses gives $P_{L_C} = 29.03$ kWh. 500 load flow simulations were performed with the tap and switch settings held at the values given in Fig. 4 and Fig. 5, but with the demand varying between 1 and 1.74 times the predicted value in a normally distributed fashion, i.e. $\alpha \leq \hat{\alpha}$. The total daily losses from each simulation were recorded and are shown in Fig. 13 as a histogram. The black dashed line shown in Fig. 13 indicates P_{L_C}, the maximum allowable loss value of 29.03 kWh. It is clear that by implementing the IGDT results for the taps and switch, the losses for all 500 simulations are kept below the desired value of 29.03 kWh.

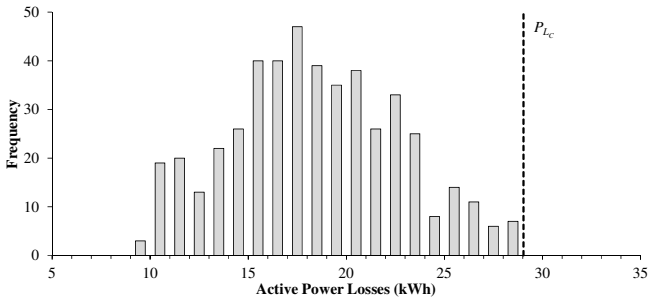

Figure 13. Histogram of losses for 500 load flow simulations using robustness settings

E. IGDT comparison with probabilistic approach

In order to perform a comparison between the proposed approach and other uncertainty formulations, a probabilistic TOPF has been performed. A probabilistic approach to this problem would require a PDF of the demand from which a number of scenarios are generated, however, since a PDF of the demand data is not available, scenarios are simulated using uniformly distributed random numbers to vary the demand between 0.2 and 2 times the predicted values. The values of 0.2 and 2 are based on the IGDT results, as well as the assumed worst case for maximum and minimum demand. Three demand scenarios are generated and a multi-scenario TOPF is performed with the same minimum loss objective and network constraints as the IGDT TOPF problem. The resulting tap and switch settings are given in Fig. 14 and Fig. 15 respectively. As the probabilistic and IGDT formulations have different aims for what the results should achieve, a direct comparison of the results for the decision variables cannot be made. The expected value of the losses in the probabilistic case is 8.16 kWh. The computation time for the three scenarios is 2641 seconds.

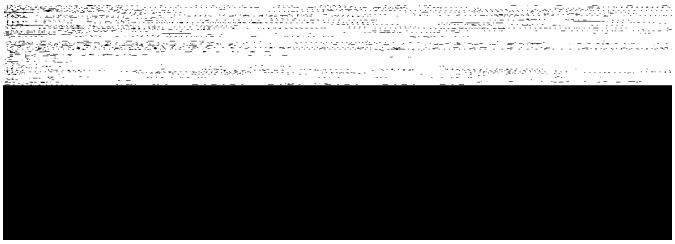

Figure 14. Feeder tap settings for phases a, b, and c for the three scenario probabilistic formulation

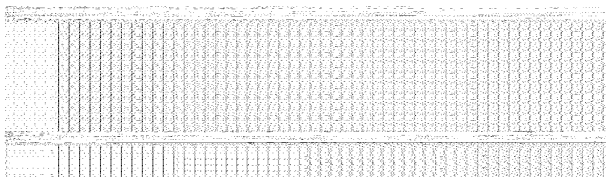

Figure 15. Switch settings for the three scenario probabilistic formulation

A new scenario is generated within the bounds of 0.2 and 2 times the predicted demand value. A load flow is performed using this demand scenario with the tap and switch settings set at the resulting values in Fig. 14 and Fig. 15. Although this scenario is within the same demand bounds as the other scenarios, using the settings from the probabilistic TOPF results in voltage limit breaches. In fact, the voltage is below the lower bound of 0.9 pu at at least one bus for 43 out of 48 time steps. Furthermore, the losses for this scenario are 15.31 kWh which is almost double the expected value. It may the case that analysing more scenarios using the probabilistic approach provides more robust decisions and a more accurate expected value. However, each probabilistic scenario adds a new dimension to the optimisation which significantly increases the size of the problem and thus the solving time. For example, when the probabilistic problem is performed with 5 scenarios the computation time increase from 2641 seconds to 7617 seconds.

The IGDT approach only requires an initial prediction of the demand. This prediction does not have to be highly accurate as the formulation deals with extreme uncertainty. The single predicted value of the IGDT method vastly reduces the computational burden of the problem in comparison to the probabilistic approach. Furthermore, as demonstrated by the validation in Section IV-D, the decisions provided by the IGDT formulation are robust for the maximum possible deviation in the demand, for a given acceptable increase in the optimal losses. In contrast, the decisions provided by the probabilistic method may not provide the same degree of robustness if specific scenarios are omitted, as the above results have demonstrated. Finally, the probabilistic technique only provides an expected value, and cannot guarantee a deterministic range for the losses. The IGDT method effectively

combats these issues by providing decisions that will be robust against extreme demand changes while maintaining losses within an acceptable range.

V. Conclusions

The work discussed here describes a novel methodology to combat the problem of uncertainties on LV distribution networks. The TOPF method accurately models three-phase networks and their associated components, as well as providing optimal solutions for distribution system control variables. The IGDT method is capable of assessing robustness and opportuneness functions for an acceptable improvement or deterioration in the objective function. This method can allow network operators to make LV network decisions that will be robust against potential deviations without adding a high level of complexity to the TOPF problem.

The formulation was tested using an actual suburban LV network to determine optimal and robust tap and switch settings. The results provide a range of operating points, with varying levels of robustness, for a network operator to choose from. Implementing the appropriate operating point from the results provided guarantees the system operator that the network losses will not exceed the desired value due to the accuracy of the three-phase modeling. The losses will also be close to or at the minimum possible value, depending on the actual demand level. This is all achieved with only a basic prediction of what the demand will be. The results shown are for one particular test network, however, the formulation can easily incorporate other networks, in both radial and meshed configuration, for the purposes of making robust decisions.

The method discussed here could be utilized for numerous planning and operational applications for distribution networks. In particular, it would be highly beneficial for the management of distributed energy resources in smart grids. The addition of distributed resources to LV networks could result in substantial increases in the level of uncertainty. The formulation described in this paper could be applied, in the same way as it is applied to load here, to provide optimal and robust operating points for these new technologies.

Appendix

Sample active and reactive power profiles for three of the customers on the feeder are given in Fig. 16. The *ZIP* load components for a customer located at node a1 in Fig. 2 are shown in Fig. 17

Cable impedance data for the test feeder shown in Fig. 2 is given in Table V.

Figure 16. Active and reactive power demand for three sample customers

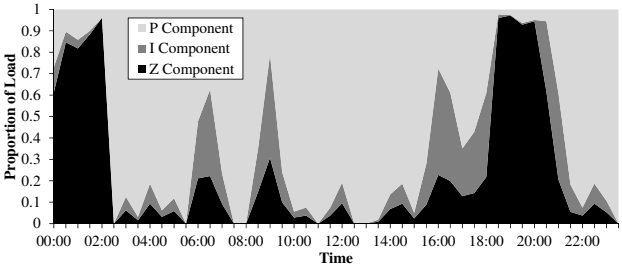

Figure 17. ZIP components for customer located at node a1 phase c

[4] P. Mirowski, S. Chen, T. K. Ho, and C.-N. Yu, "Demand forecasting in smart grids," *Bell Labs Technical Journal*, vol. 18, no. 4, pp. 135–158, 2014.

[5] S. Sarhadi and T. Amraee, "Robust dynamic network expansion planning considering load uncertainty," *Int. J. Elect. Power & Energy Syst.*, vol. 71, pp. 140–150, 2015.

[6] P. Caramia, G. Carpinelli, M. Pagano, and P. Varilone, "Probabilistic three-phase load flow for unbalanced electrical distribution systems with wind farms," *IET Renewable Power Generation*, vol. 1, no. 2, pp. 115–122, 2007.

[7] B. Das, "Consideration of input parameter uncertainties in load flow solution of three-phase unbalanced radial distribution system," *IEEE Trans. Power Syst.*, vol. 21, no. 3, pp. 1088–1095, 2006.

[8] A. O'Connell, D. Flynn, and A. Keane, "Rolling multi-period optimization to control electric vehicle charging in distribution networks," *IEEE Trans. Power Syst.*, vol. 29, no. 1, pp. 340–348, 2014.

[9] Y. Cao, Y. Tan, C. Li, and C. Rehtanz, "Chance-constrained optimization-based unbalanced optimal power flow for radial distribution networks," *IEEE Trans. Power Del.*, vol. 28, no. 3, pp. 1855–1864, 2013.

Table V
Test feeder cable data

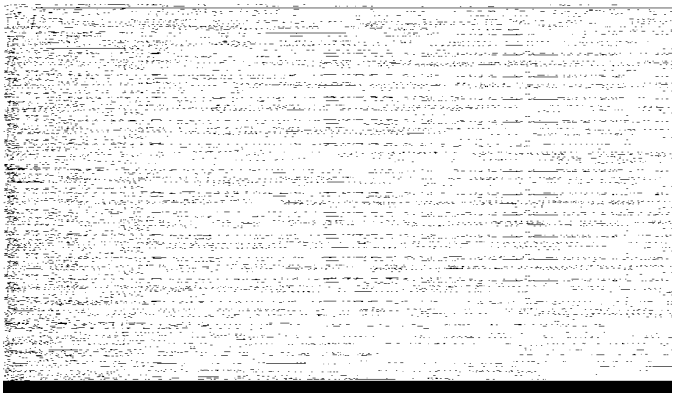

References

[1] P. Richardson, M. Moran, J. Taylor, A. Maitra, and A. Keane, "Impact of electric vehicle charging on residential distribution networks: an Irish demonstration initiative," in *Proc. CIRED 22nd Int. Conf. on Electricity Distribution*, 2013.

[2] Green eMotion Project. [Online]. Available: http://www.greenemotion-project.eu/

[3] L. Ochoa and P. Mancarella, "Low-carbon LV networks: Challenges for planning and operation," in *Proc. IEEE Power and Energy Society GM*, 2012.

[10] G. K. Viswanadha Raju and P. R. Bijwe, "Reactive power/voltage control in distribution systems under uncertain environment," *IET Generation, Transmission & Distribution*, vol. 2, no. 5, pp. 752–763, 2008.

[11] A. Soroudi, "Possibilistic-scenario model for DG impact assessment on distribution networks in an uncertain environment," *IEEE Trans. Power Syst.*, vol. 27, no. 3, pp. 1283–1293, 2012.

[12] Y. Deng and X. Ren, "Fuzzy modeling of capacitor switching for radial distribution systems," in *Power Engineering Society Winter Meeting, 2001. IEEE*, vol. 2, 2001, pp. 830–834.

[13] Y. Ben-Haim, *Info-Gap Decision Theory*, 2nd ed. Academic Press, 2006.

[14] M. A. McCarthy and D. B. Lindenmayer, "Info-gap decision theory for assessing the management of catchments for timber production and urban water supply," *Environmental Management*, vol. 39, no. 4, pp. 553–562, 2007.

[15] D. R. Harp and V. V. Vesselinov, "Contaminant remediation decision analysis using information gap theory," *Stochastic Environmental Research and Risk Assessment*, vol. 27, no. 1, pp. 159–168, 2013.

[16] D. Hine and J. W. Hall, "Information gap analysis of flood model uncertainties and regional frequency analysis," *Water Resources Research*, vol. 46, no. 1, 2010.

[17] B. Beresford-Smith and C. J. Thompson, "Managing credit risk with info-gap uncertainty," *The Journal of Risk Finance*, vol. 8, no. 1, pp. 24–34, 2007.

[18] J. Zhao, C. Wan, Z. Xu, and J. Wang, "Risk-based day-ahead scheduling of electric vehicle aggregator using information gap decision theory," *IEEE Trans. Smart Grid*, vol. PP, no. 99, pp. 1–10, 2015.

[19] C. Murphy, A. Soroudi, and A. Keane, "Information gap decision theory-based congestion and voltage management in the presence of uncertain wind power," *IEEE Trans. Sustainable Energy*, vol. PP, no. 99, pp. 1–9, 2015.

[20] A. Soroudi and M. Ehsan, "IGDT based robust decision making tool for DNOs in load procurement under severe uncertainty," *IEEE Trans. Smart Grid*, vol. 4, no. 2, pp. 886–895, 2013.

[21] A. O'Connell and A. Keane, "Multi-period three-phase optimal power flow," in *Innovative Smart Grid Technologies Europe*, 2014.

[22] Y. Ben-Haim, "Uncertainty, probability and information-gaps," *Rel. Eng. and Syst. Safety*, vol. 85, no. 1–3, pp. 249–266, 2004.

[23] A. J. Collin, G. Tsagarakis, A. E. Kiprakis, and S. McLaughlin, "Development of low-voltage load models for the residential load sector," *IEEE Trans. Power Syst.*, vol. 29, no. 5, pp. 2180–2188, 2014.

[24] B. Stott and O. Alsac, *White Paper: Optimal Power Flow - Basic Requirements for Real-Life Problems and their Solutions*, 2012. [Online]. Available: http://www.ieee.hr/_download/repository/Stott-Alsac-OPF-White-Paper.pdf

[25] C. Dent, L. Ochoa, and G. Harrison, "Network distributed generation capacity analysis using OPF with voltage step constraints," *IEEE Trans. Power Syst.*, vol. 25, no. 1, pp. 296–304, 2010.

[26] AIMMS 3.13. [Online]. Available: http://business.aimms.com/

[27] CONOPT. [Online]. Available: http://www.conopt.com/

[28] ESB Networks. [Online]. Available: http://www.esb.ie/esbnetworks/en/home/index.jsp

[29] K. McKenna and A. Keane, "Residential load modeling of price based demand response for network impact studies," *IEEE Trans. Smart Grid*, vol. PP, no. 99, 2015.

[30] P. Siano, "Demand response and smart grids - a survey," *Renewable and Sustainable Energy Reviews*, vol. 30, pp. 461–478, 2014.

[31] A. Soroudi and M. Afrasiab, "Binary pso-based dynamic multi-objective model for distributed generation planning under uncertainty," *IET Renewable Power Generation*, vol. 6, no. 2, pp. 67–78, 2012.

Alison O'Connell (S'12) received both the B.E. and Ph.D. degrees in Electrical Engineering from University College Dublin in 2011 and 2015, respectively. She is currently a Senior Energy System Researcher at University College Dublin with the Electricity Research Centre. Her research interests include distribution network modelling, unbalanced load flow and distributed energy resources.

Alireza Soroudi (M'14) Received the B.Sc. and M.Sc. degrees from Sharif University of Technology, Tehran, Iran, in 2002 and 2004, respectively, both in electrical engineering. and the joint Ph.D. degree from Sharif University of Technology and the Grenoble Institute of Technology (Grenoble-INP), Grenoble, France, in 2011. He is the winner of the ENRE Young Researcher Prize at the INFORMS 2013. He is currently a senior researcher with the School of Electrical, Electronic, and Mechanical Engineering, University College Dublin with research interests in uncertainty modeling and optimization techniques applied to Smart grids, power system planning and operation.

Andrew Keane (S'04–M'07–SM'14) received the B.E. and Ph.D. degrees in electrical engineering from University College Dublin, Ireland, in 2003 and 2007, respectively. He is currently Head of School and a Senior Lecturer with the School of Electrical and Electronic Engineering, University College Dublin. He has previously worked with ESB Networks, the Irish Distribution System Operator. His research interests include power systems planning and operation, distributed energy resources, and distribution networks.